Molecular Neurobiology
https://doi.org/10.1007/s12035-024-04016-8

ORIGINAL ARTICLE

Transcriptomics and Metabolomics Unveil the Neuroprotection Mechanism of AnGong NiuHuang (AGNH) Pill Against Ischaemic Stroke Injury

Liangliang Tian[1] · Guangzhao Cao[1,2] · Xiaotong Zhu[1] · Lihan Wang[2] · Jingyi Hou[2] · Yi Zhang[1] · He Xu[1] · Lixia Wang[1] · Shicong Wang[3] · Chen Zhao[3] · Hongjun Yang[1,2] · Jingjing Zhang[1,4]

Received: 16 November 2023 / Accepted: 2 February 2024

Abstract

As a famous prescription in China, AnGong NiuHuang (AGNH) pill exerts good neuroprotection for ischaemic stroke (IS), but its mechanism is still unclear. In this study, the neuroprotection of AGNH was evaluated in the rat IS model which were established with the surgery of middle cerebral artery occlusion (MCAO), and the potential mechanism was elucidated by transcriptomic analysis and metabolomic analysis. AGNH treatment obviously decreased the infarct volume and Zea-Longa 5-point neurological deficit scores, improved the survival percentage of rats, regional cerebral blood flow (rCBF), and rat activity distance and activity time. Transcriptomics showed that AGNH exerted its anti-inflammatory effects by affecting the regulatory network including Tyrobp, Syk, Tlr2, Myd88 and Ccl2 as the core. Integrating transcriptomics and metabolomics identified 8 key metabolites regulated by AGNH, including L-histidine, L-serine, L-alanine, fumaric acid, malic acid, and N-(L-arginino) succinate, 1-pyrroline-4-hydroxy-2-carboxylate and 1-methylhistamine in the rats with IS. Additionally, AGNH obviously reduced Tyrobp, Syk, Tlr2, Myd88 and Ccl2 at both the mRNA and protein levels, decreased IL-1β, KC-GRO, IL-13, TNF-α, cleaved caspase 3 and p65 nucleus translocation, but increased IκBα expression. Network pharmacology analysis showed that quercetin, beta-sitosterol, baicalein, naringenin, acacetin, berberine and palmatine may play an important role in protecting against IS. Taken together, this study reveals that AGNH reduced neuroinflammation and protected against IS by inhibiting Tyrobp/Syk and Tlr2/Myd88, as well as NF-κB signalling pathway and regulating multiple metabolites.

Keywords Cerebral ischaemia · Tyrobp · Inflammation · Syk · Tlr2 · Myd88

Abbreviations

IS	Ischaemic stroke
AD	Alzheimer disease
AGNH	AnGong NiuHuang
BBB	Blood-brain barrier
DEGs	Differentially expressed genes
DMs	Differentially expressed metabolites
ELISA	Enzyme-linked immunosorbent assay
GO	Gene Ontology
rCBF	Regional cerebral blood flow
I/R	Ischaemia/reperfusion
IF	Immunofluorescence staining
KEGG	Kyoto Encyclopedia of Genes and Genomes
MCAO	Middle cerebral artery occlusion
SD	Sprague-Dawley
TCM	Traditional Chinese medicine
TTC	2,3,5-Triphenyltetrazolium chloride
Ccl2	C-C motif chemokine ligand 2
Tlr2	Toll-like receptor 2
Tlr7	Toll-like receptor 7
Myd88	Myeloid differentiation factor 88
Tyrobp	TYRO protein tyrosine kinase-binding protein
Syk	Spleen tyrosine kinase

Introduction

Ischaemic stroke (IS), caused by cerebral blood vessel occlusion, leads to brain damage due to the decline in the supply of oxygen and glucose, which results in many long-term disabilities and large mortality rates worldwide [1, 2]. Besides anticoagulant therapy, effective treatment strategies for IS are limited. In particular, restoring blood flow by

Liangliang Tian and Guangzhao Cao contributed equally to this work.

Extended author information available on the last page of the article

Published online: 24 February 2024

using recombinant tissue-type plasminogen activator (rtPA) often exacerbates cerebral ischaemia damage, and this process is called ischaemia/reperfusion (I/R) damage [3, 4]. As ischaemia is initiated in the brain, rapid cell death occurs in the ischaemic region, whereas neurons in the peri-infarct region can be protected and survive the event. Preserving these peri-infarct neurons is important for the prognosis and recovery of IS patients. In particular, cerebral ischaemia is a complex and complicated disease closely related to multiple pathological processes, such as overproduction of free radicals, destruction of the blood–brain barrier (BBB), energy metabolism disorder, excitatory amino acid toxicity and inflammation, which interact with each other and cause a vicious feedback cycle, eventually leading to neuronal death and brain damage [5]. These effects highlight the importance of searching for therapeutic treatments to minimize brain damage and offer effective neuroprotection during IS.

Traditional Chinese medicine (TCM) shows great potential for treating IS since it displays good efficacy and few side effects [6, 7]. Our previous studies indicated that Guhong injection protected against cerebral ischaemia injury by restoring antioxidant Nrf2, Trx and GSH systems at the start of reperfusion [8] and suppressed inflammation by inhibiting C5AR1 for a relatively prolonged time period [9]. Another study showed that Duzhi Wan decreased C3 and C5 levels to inhibit inflammation and offered neuroprotective effects against cerebral I/R [6]. Additionally, Dengzhan Shengmai capsule improved neurological function and decreased the recurrence of IS [10, 11].

As a famous Chinese medicine product, AnGong NiuHuang (AGNH) pill is recorded in Chinese pharmacopoeia [12] and used for cerebrovascular diseases including IS for a long time [13, 14]. The use of AGNH can trace its history back to seventeenth century (Qing dynasty) in China. AGNH is consisted of Cinnabaris (100 g), Bovis Calculus Sativus (100 g), Powdered Buffalo Horn Extract (200 g), *Hyriopsis cumingii* (Lea) (50 g), Artificial Moschus (25 g), *Curcuma aromatica* Salisb. (100 g), *Scutellaria baicalensis* Georgi (100 g), *Gardenia jasminoides* J.Ellis (100 g), Borneolum Syntheticum (25 g), *Coptis chinensis* Franch (100 g) and Realgar (100 g). AGNH is widely used in clinic in China, and also proved to have good protection for IS patients and middle cerebral artery occlusion (MCAO) IS animal model [15, 16]. A meta-analysis study of 1601 patients demonstrated AGNH can decrease neurologic deficit score of IS patients in randomized controlled trials [15]. Another study has shown that AGNH reduced infarct size and preserved the BBB integrity in MCAO rats while it did not affect liver and kidney functions after 1 week's administration [16]. Besides, combined application of AGNH and t-PA significantly reduced mortality rate and brain oedema, decreased BBB damage and prevented haemorrhagic transformation through reducing MMP9 activation in MCAO rats, when compared with the only treatment of t-PA [17]. In an mouse IS model, AGNH was reported to regulate gut microbiota dysbiosis to alleviate brain injury and cell apoptosis [18]. Though several studies have been reported about the protective effect of AGNH on IS, the underlying mechanism remains unclear and needs to be investigated.

With the development of technology, the mechanisms of TCM can be holistically revealed by using high-throughput multiomics data [19]. In this study, MCAO surgery was used to induce cerebral I/R damage, and the effects of AGNH on MCAO-induced cerebral ischaemia damage in rats were evaluated. Multiple modes of administration of AGNH provide more deep understanding of the effect of AGNH on ischaemic stroke and help the clinical application of AGNH in IS treatment. And transcriptomic analysis and metabolomics analysis were integrated to investigate the mechanism.

Materials and Methods

Animal Experiments

Beijing Charles River Experimental Animal Technology Co., Ltd offered male specific pathogen-free (SPF) Sprague–Dawley (SD) rats (280 ~ 320 g) [(certificate no. SCXK (Jing) 2014–0004)]. A room with a 12-h light/dark cycle was used for the keeping rat. During the experiments, these rats were kept to be allowed to drink and eat freely in a room with a temperature of 22–26 °C. The AGNH pill used in our experiment was provided by Zhangzhou Pien Tze Huang Pharmaceutical Co., Ltd.

We conducted MCAO surgery to induce cerebral ischaemia in SD rats after anaesthetization with sodium pentobarbital (i.p.). A nylon thread of 4–0 was used to block the internal carotid artery (ICM) for 90 min and then released to restore blood flow. At the same time, the rats were kept at 37 °C to maintain their body temperature and protect against hypothermia. Briefly, 128 SD rats were used in our experiments and 114 rats were received MCAO surgery. Then, the MCAO subjected rats were evaluated by using neurological deficient score and the rats with neurological deficient score no less than 1 were supposed to be ischaemic stroke and were randomly divided into the I/R group (receiving physiological saline), I/R + AGL (0.09 g•kg^{-1} AGNH), I/R + AGH (0.27 g•kg^{-1} AGNH, the clinical equivalent dose) and I/R + Ginaton (8 mL·kg^{-1} Ginaton) by using a random number table. Ginaton is extract of the *Ginkgo biloba* leaves and is mainly used for cerebral and peripheral blood circulation disorders, such as ischaemic stroke [20, 21]. In this study, Ginaton was used as a positive control for the neuroprotection investigation of AGNH on MCAO rat model. The rats were subjected for 1.5 h MCAO-caused ischaemia and followed by 5 days' reperfusion. During the reperfusion, the rats were given

daily AGNH for 5 consecutive days (Fig. 1A). All drugs were administered through intragastric administration. The same operation was conducted in the rats of the sham group except for blocking the blood flow by inserting the thread. Finally, the rats were evaluated using the Zea-Longa 5-point neurological deficit scale and then sacrificed to harvest tissue and serum for the following experiments.

Survival Percentage and Zea-Longa 5-Point Neurological Deficit Score Detection

The survival number of the rats in the experiment was recorded, and the survival percentage was obtained by normalizing the number of surviving rats to the number of overall rats. Neurological function deficits were assessed by using the Zea-Longa 5-point neurological deficit scale, which includes five grades for scoring. These grades were as follows: score 0 point, walking normally; score 1, unable to walk straight and slight forelimb weakness; score 2 point, circling to the paralysed side, severe weakness of the forelimb; score 3 point, cannot stand and fall to the paralysed side; score 4 point, no autonomous walking and low level of consciousness; and score 5 point, death.

Regional Cerebral Blood Flow (rCBF) Testing and 2,3,5-Triphenyltetrazolium Chloride (TTC) Staining

For rCBF testing, the rats with various treatments were anaesthetized, and then the rCBF of rat brains was evaluated using laser Doppler flowmetry. The rCBF was calculated with the related analysis system. After sacrificing the rats, the brains were harvested and cut into 2-mm sections for staining with 2% (w/v) TTC. Afterwards, the brain sections were incubated with paraformaldehyde for fixation. The infarct volume was obtained by normalizing the infarcted area of the rat brain to its overall area.

Open Field Test

After administration of AGNH for 5 days, the rats were evaluated using the open field test to observe their autonomous behaviour and exploratory behaviour. The entire open field experiment system consists of an open field box, a camera system and video recording and analysis software. The open box shape can be square, rectangular or round. A 100 cm*100 cm*50 cm open field box was used in our experiment. The rats were placed in a specific position in the open box, and the camera system was used to monitor the animals' activities in the open box. VisuTrack video recording and analysis software (Shanghai Xinruan) was used to track the animals' activity tracks and collect and analyse data. The activity of rats is reflected by comparing the total moving distance and total activity time of rats.

Transcriptomics Analysis

The RNA extracted from rat brains with various treatments was used for cDNA library construction on the Illumina NovaSeq platform before the RNA quality was evaluated and purification was finished according to previous protocols [9]. Novogene Bioinformatics Technology Co., Ltd. completed the RNA library construction, sequencing and mapping by using 150-bp paired-end reads. The mapping was finished by using version of ensemble release 91 of rat reference genome. The genes that were belonged to $|\log_2 \text{fold change}| \geq 1$ with the *Padj* less than 0.05 in the DEseq2 R package (1.20.0) were supposed to differentially expressed (DEGs). The enrichment of DEGs was performed with the Metascape and DAVID databases. The raw data of AGNH-based RNA-seq analysis have been uploaded into the NCBI database of https://www.ncbi.nlm.nih.gov/bioproject/PRJNA913295. The DEGs are listed in Table S1.

Immunofluorescence Staining (IF), Western Blotting Experiments and Enzyme-Linked Immunosorbent Assay (ELISA)

After AGNH treatment, the harvested rat brains were fixed with polyformaldehyde, followed by ethanol for dehydration, and then paraffin was used to embed these brains. Brain sections that were 5 μm thick were prepared for subsequent staining. Specifically, antigen repair was performed by incubating the sections with sodium citrate buffer solution and then the sections were permeabilized with Triton X-100. Next, bovine serum albumin was incubated with the sections to block background endogenous peroxidases. Primary antibodies such as NeuN (ab104224), IBA-1 (GB12105), cleaved caspase 3 (CST 9664) and p65 (CST, 8242S) were incubated with the brain sections to identify the target proteins, and secondary antibodies such as Alexa Fluor 488-conjugated antibody or Alexa Fluor 647 antibody were incubated with the sections to visualize the target protein. Additionally, staining cell nuclei with DAPI for 20 min, and then photos were taken by using an LSM-880 confocal microscope.

First, we homogenized the rat brain with RIPA buffer, and then added the phosphatase and protease inhibitors to the brain mixture. The extracted protein from brain was quantified with BCA protein kit (ab102536). Briefly, the 12% SDS-PAGE was used to separate the protein which was then transferred to PVDF membrane (0.45 μm). After that, the membrane was blocked with 5% milk for 120 min, and then the primary antibodies such as IκBα (1:1000, Abcam, ab76429) were incubated with the membrane overnight at 4 °C, respectively. The anti-rabbit IgG (Abcam 205,718) was added to the membranes for 2 h and an enhanced chemiluminescence (ECL) western blot detection system was applied to detect the protein signals. ELISA was conducted and detected in a microplate reader (DNM-9602G) according to the kits' instructions. The value

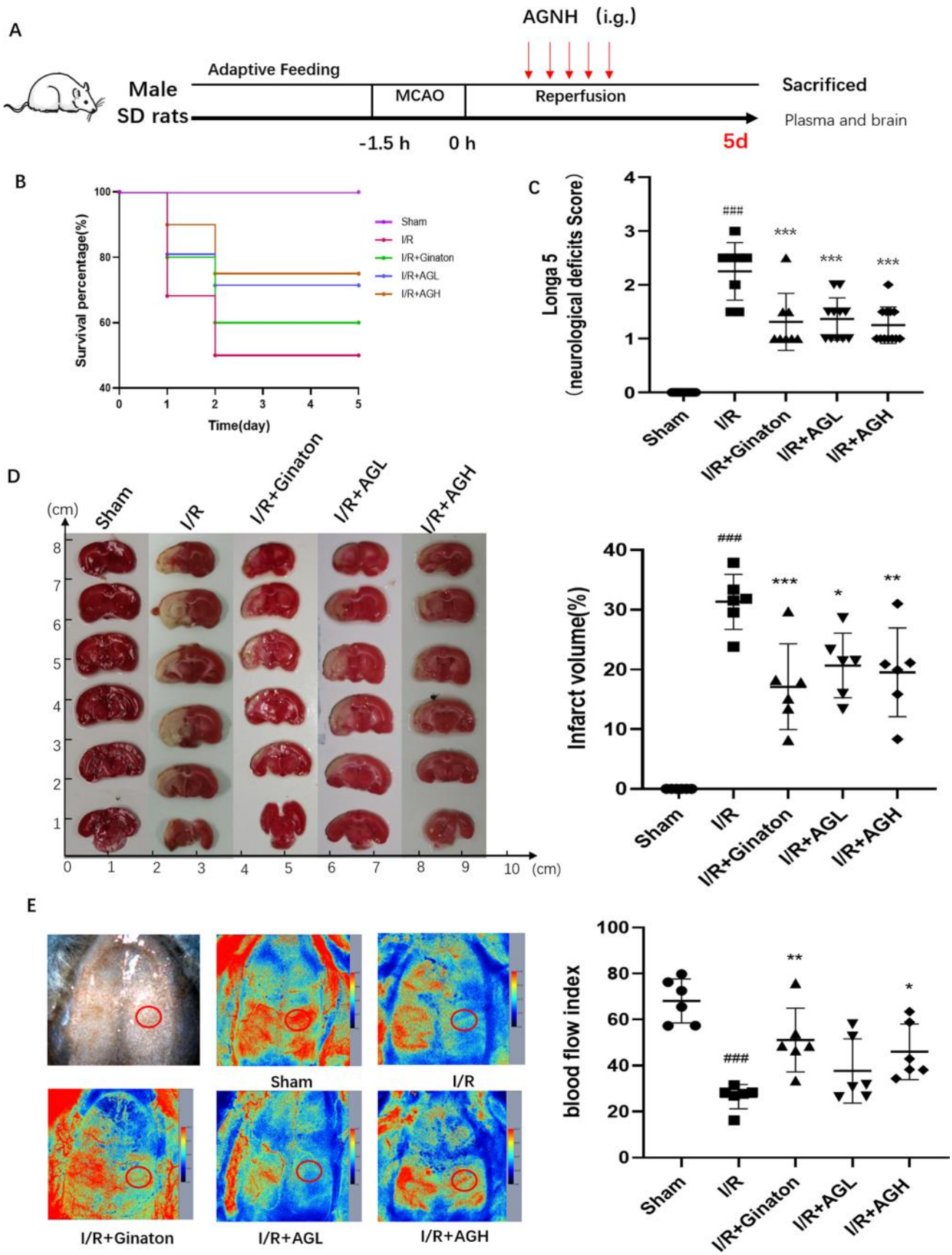
A
AGNH (i.g.)
Adaptive Feeding
Male
SD rats
MCAO
Reperfusion
Sacrificed
Plasma and brain
-1.5 h
0 h
5d
B
Survival percentage(%)
Time(day)
Sham
I/R
I/R+Ginaton
I/R+AGL
I/R+AGH
C
Longa 5
(neurological deficits Score)
###
***
***
***
Sham
I/R
I/R+Ginaton
I/R+AGL
I/R+AGH
D
(cm)
Sham
I/R
I/R+Ginaton
I/R+AGL
I/R+AGH
Infarct volume(%)
###
***
*
**
E
Sham
I/R
I/R+Ginaton
I/R+AGL
I/R+AGH
blood flow index
**
###
*

◂**Fig. 1** Treatment with AGNH for 5 days decreased I/R injury in MCAO rats. **A** Experimental design; **B** survival percentage ($n = 16$–32); **C** Zea-Longa 5-point scores ($n = 8$–11); **D** TTC images of brain sections and the calculated infarct volume ($n = 6$); **E** rCBF of rats after various treatments ($n = 6$); $^{\#\#\#}p < 0.001$ vs. sham, $^{*}p < 0.05$, $^{***}p < 0.001$ vs. I/R group

was calculated based on its standard curve depending on the ELISA kits. Tyrobp (RTEB0822) and Syk (TW990223) kits were obtained from Wuhan Abebio Science Co., Ltd. and Shanghai Tongwei Co., Ltd., respectively. Tlr2 (SEB663Ra) and Myd88 (SEB707Ra) kits were obtained from Cloud-Clone Corp. (Wuhan), a Tlr7 (ELK8392) kit was obtained from ELK Biotechnology Co., Ltd., and a Ccl2 (E-EL-R0633c) kit was obtained from Elabscience Biotechnology Co., Ltd. These kits were used to measure Tyrobp, Syk, Tlr2, Myd88, Tlr7 and Ccl2 levels, respectively.

Inflammatory Cytokine Chip Detection

Proinflammatory panel 2, including 9 cytokines, such as IL-1β, IL-4, IFN-γ, IL-6, KC/GRO, IL-5, IL-13, IL-10 and TNF-α, was detected with the electrochemiluminescence method by using a Meso Scale Discovery (MSD) hypersensitive multifactor electrochemiluminescence analyser (Meso QuickPlex SQ 120).

Untargeted Metabolomics Analysis Based on UHPLC-MS/MS Analysis

The brain in rats treated with a high dose of AGNH was used for metabolomics analysis. Briefly, the rat brain tissue from various groups was extracted by using methanol solution and the extract was centrifuged at 13,000 g at 4 °C for 15 min. After that, the UHPLC-Q Exactive system (Thermo Fisher Scientific) was used for the following LC–MS analysis with an HSS T3 column with100 mm × 2.1 mm i.d., 1.8 μm. During the experiments, the mobile phases included solvent A and solvent B. The solvent A is 0.1% formic acid in water:acetonitrile (95:5, v/v). The solvent B is 0.1% formic acid in acetonitrile:isopropanol:water (47.5:47.5:5, v/v). The solvent gradient was set depending on the time change as follows: 0–0.1 min, 0–5% solvent B; 0.1–2 min, 5–25% solvent B; 2–9 min, 25–100% solvent B; 9–13 min, 100% solvent B; 13–13.1 min, 100–0% solvent B; and 13.1–16 min, 0% solvent B. The temperature of capillary and heater was 320 °C and 400 °C, respectively. And the aux gas flow rate and sheath gas flow rate were 10 arb and 40 arb, respectively. The other conditions were listed as following contents: ion-spray voltage floating (ISVF), 3500 V in positive mode and − 2800 V in negative mode. The differential metabolites (DMs) were identified by using variable importance in the projection (VIP) at a value larger than 1, which was analysed with the OPLS-DA model, and a p value at a value less than 0.05, according to Student's t-test (Table S2). The enriched metabolic pathways with p adjust value less than 0.05 was supposed to important metabolic pathways and were presented in Fig. 3D.

Integrating Data from Transcriptomics and Metabolomics

The DMs from metabolomics and DEGs from transcriptomics were integrated by using Metscape in Cytoscape 3.9.0 using the pathway-based model. And the vital metabolic pathways were further identified after integrating these two omics data. To further understanding the mechanism, a network of DEGs in vital metabolic pathways such as TCA, histidine metabolism, glycerophospholipid metabolism, urea cycle and metabolism of arginine, proline, glutamate, aspartate and asparagine (Fig. 5A–D) were associated with the DEGs enriched in inflammatory response by using STRING database with the score no less than 0.4 and interaction between targets was then visualized by using Cytoscape 3.9.0

Heterogeneous Network Construction by Using Network Pharmacology Analysis

The components of AGNH were collected from database of Traditional Chinese Medicine System Pharmacological Analysis platform (TCMSP, https://tcmspw.com/tcmsp.php) and the components with oral bioavailability (OB) ≥ 30% and drug like properties (DL) ≥ 0.18 were supposed to be potential components for following analysis. Then, the corresponding targets were predicted for the screened components and the protein target information was standardized and unified in the Uniprot protein database (https://www.uniprot.org). The drug targets were associated with the AGNH-regulated DEGs that were involved in inflammatory response and the metabolic pathways of TCA, histidine metabolism, glycerophospholipid metabolism, urea cycle and metabolism of arginine, proline, glutamate, aspartate and asparagine, by using STRING database (https://string-db.org) with the confidence score no less than 0.7. And the drug targets that were associated with AGNH-regulated DEGs were screened out and then the corresponding components were then identified. Finally, the heterogeneous network of components-drug target-AGNH regulated DEGs was built with Cytoscape 3.7.0 software.

Statistical Analysis

We used t-test to analyse the obtained data between two groups and one-way ANOVA with SPSS 22.0 software was applied to analyse the results from multiple groups. The homogeneity of variance was evaluated with Levene before multiple comparison of different groups. LSD test was used for homogeneous variance, and Dunnett's T3 test was used for uneven variance. The p value less than 0.05 was considered as significance. The results are shown as the mean ± standard deviation (SD). $^{\#}p < 0.05$,

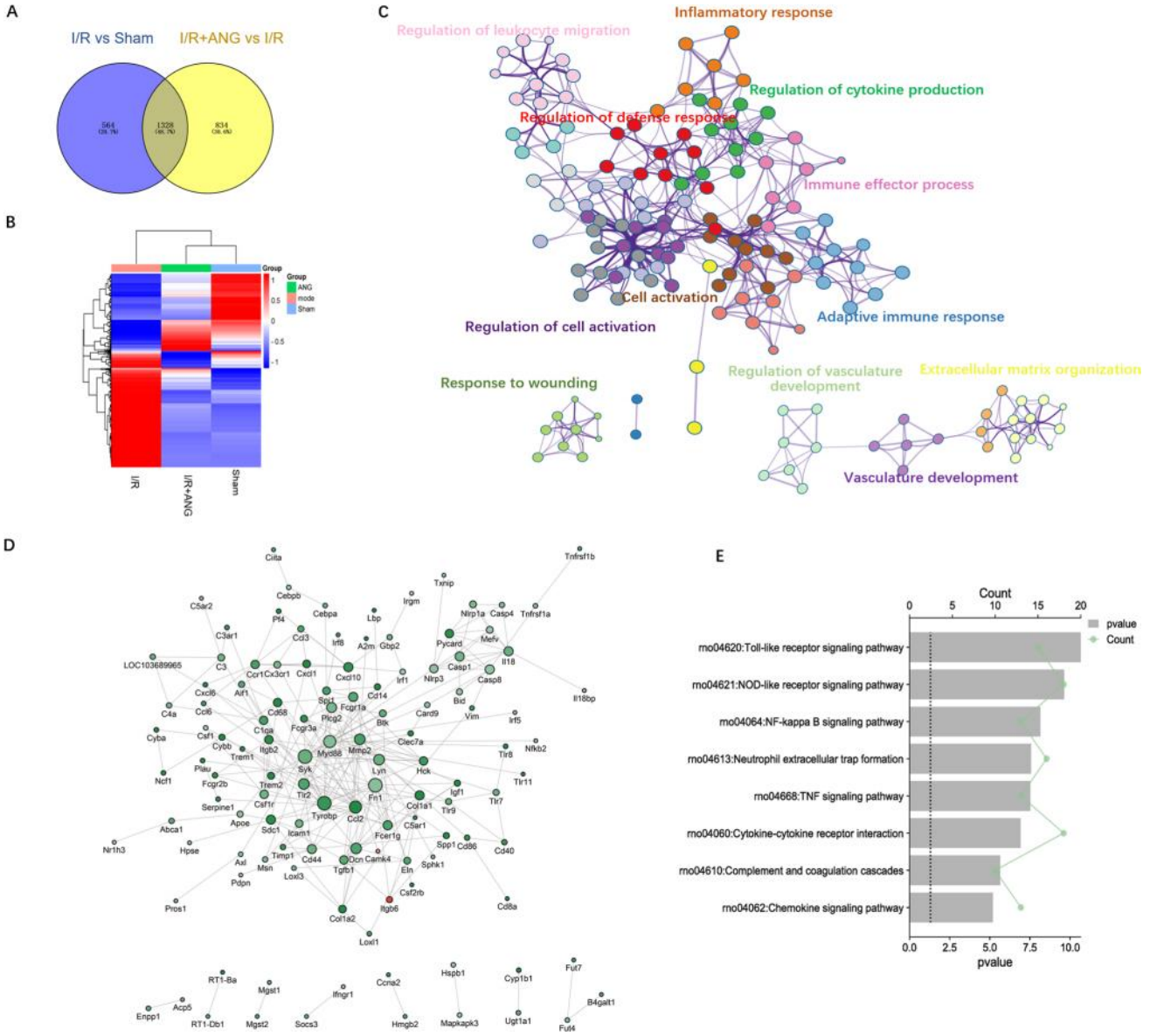

Fig. 2 The transcriptomic results of gene expression alteration caused by AGNH treatment after I/R; (**A**) Venn diagram of various groups; (**B**) hierarchical heatmap of sham, I/R and I/R + ANH group; (**C**) GO enrichment of shared DEGs of I/R vs. sham and I/R + AGH vs. I/R. (**D**) Network of the DEGs enriched in the GO term "inflammatory response", downregulated DEGs (green nodes); upregulated DEGs (red nodes); (**E**) the enriched KEGG pathways of the DEGs involved in the "inflammatory response" process

$^{\#\#}p < 0.01$, $^{\#\#\#}p < 0.001$ vs. sham, and $^{*}p < 0.05$, $^{**}p < 0.01$, $^{***}p < 0.001$ vs. I/R represented significance of the data.

Results

AGNH Protected Rats Against MCAO-Induced Cerebral Damage

AGNH is a famous Chinese medicine product approved by Chinese government to treat cerebral ischaemia [12]. Baicalin and berberine hydrochloride, which are the important components in AGNH [12], can be found in rat plasma after intragastrical administration of AGNH (Fig. S1). Importantly, rats subjected to MCAO surgery after 5 days of reperfusion displayed obvious damage to the brain, as indicated by increased neurological deficit scores (2.25 ± 0.53, $p < 0.001$) and infarct volume ($31.46 \pm 4.62\%$, $p < 0.001$), as well as decreased survival percentage of the rats to 68% at day 1 (Fig. 1A–D). In contrast, treatment of AGNH at the low and high dose significantly decreased the infarct volume to $20.69 \pm 5.41\%$

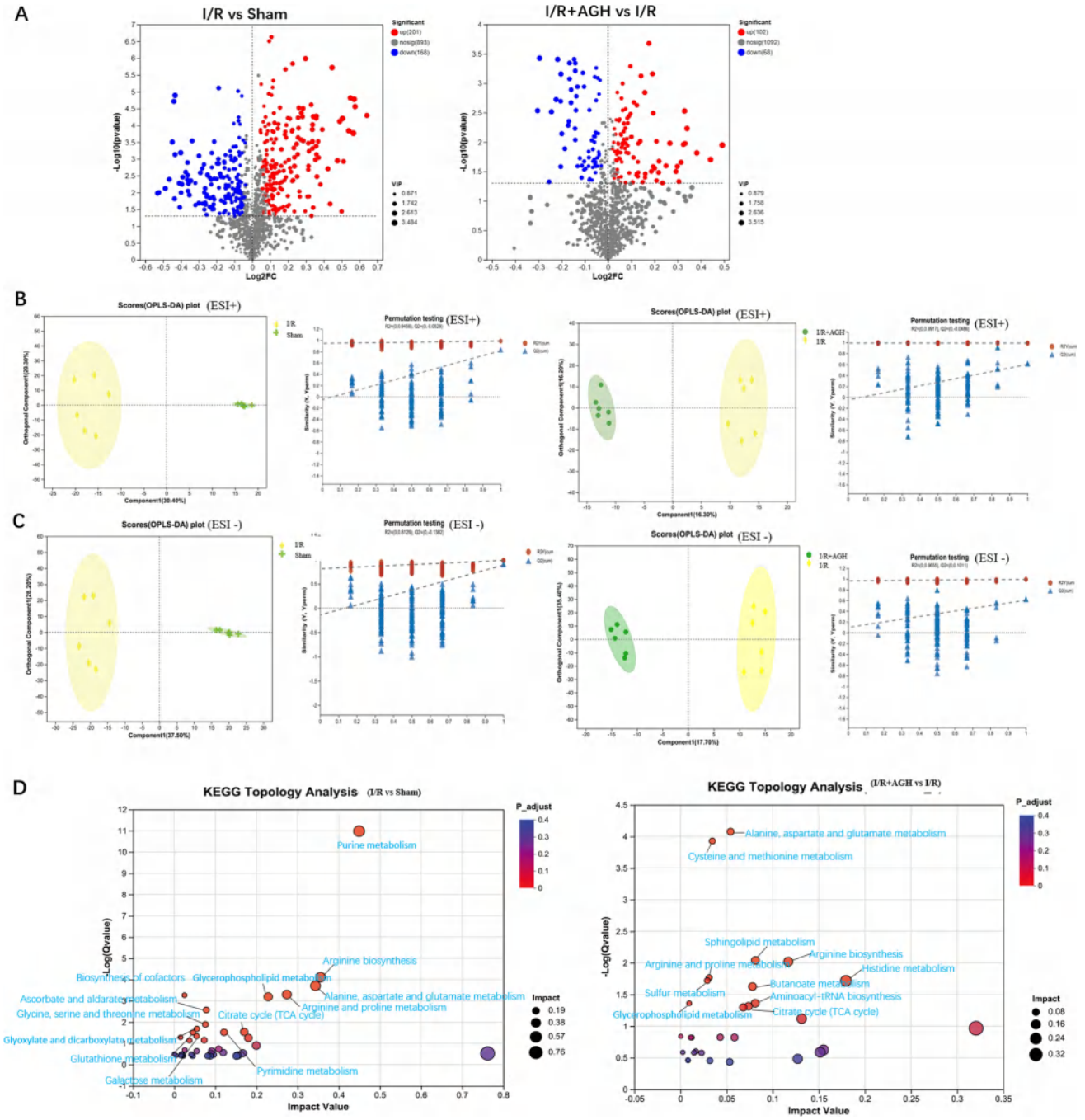

Fig. 3 Metabolic signatures of various treatments; (**A**) volcano plots; (**B**) OPLS-DA and permutation scores in the positive mode; (**C**) OPLS-DA and permutation scores in the negative mode; (**D**) KEGG topology analysis between various treatments and the enriched pathways with the *padj* < 0.05 were shown ($n = 6$)

($p < 0.05$) and $19.54 \pm 7.42\%$ ($p < 0.001$), decreased the Zea-Longa 5-point neurological deficient scores to 1.36 ± 0.39 ($p > 0.05$) and 1.25 ± 0.34 ($p < 0.05$), and increased the rat survival percentage to 80% and 90% at day 1, respectively. Moreover, MCAO surgery led to a sharp decrease in rCBF ($p < 0.001$), whereas treatment of AGNH at high dose significantly increased rCBF ($p < 0.05$) (Fig. 1E). These results indicated that AGNH treatment exerted good neuroprotection against MCAO-induced rat brain injury.

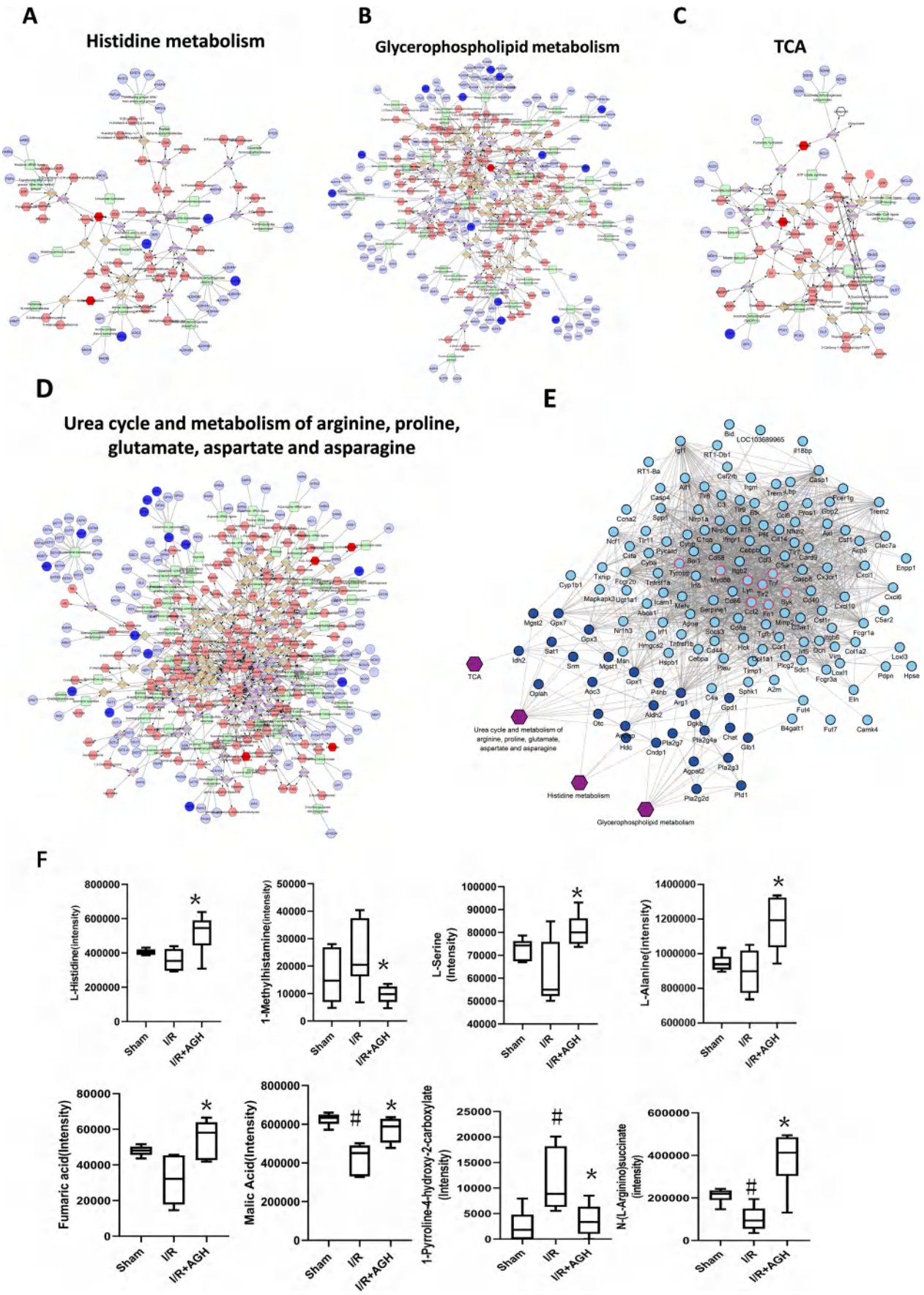
A
Histidine metabolism
B
Glycerophospholipid metabolism
C
TCA
D
Urea cycle and metabolism of arginine, proline, glutamate, aspartate and asparagine
E
TCA
Urea cycle and metabolism of arginine, proline, glutamate, aspartate and asparagine
Histidine metabolism
Glycerophospholipid metabolism
F
L-Histidine(intensity)
1-Methylhistamine(intensity)
L-Serine (Intensity)
L-Alanine(intensity)
Fumaric acid(Intensity)
Malic Acid(Intensity)
1-Pyrroline-4-hydroxy-2-carboxylate (Intensity)
N-(L-Arginino)succinate (intensity)
Sham
I/R
I/R+AGH

◂**Fig. 4** The compound-reaction-enzyme-gene network of the key metabolites and the involved DEGs in these metabolic pathways by integrating the data from transcriptomics and metabolomics; (**A**) histidine metabolism, (**B**) glycerophospholipid metabolism, (**C**) TCA, (**D**) urea cycle and metabolism of arginine, proline, glutamate, aspartate and asparagine; compounds (hexagons), reactions (grey diamonds), proteins (green round rectangle), genes (purple circles), DMs (red hexagons), DEGs (dark blue circles); (**E**) the DEGs enriched in inflammatory response (light blue circles) were closely associated with the DEGs involved in the identified metabolomic pathways (dark blue circles), the light blue circles with red frame were supposed to be the core targets identified by transcriptomics analysis in Fig. 2. (**F**) Key DMs in histidine metabolism, glycerophospholipid metabolism, urea cycle and metabolism of arginine, proline, glutamate, aspartate and asparagine and TCA, $^{\#}p < 0.05$ vs. sham; $^{*}p < 0.05$ vs. I/R group ($n = 6$)

Transcriptomic Analysis

To reveal the neuroprotective mechanism of AGNH, RNA-seq analysis was applied to probe the gene expression profile of MCAO-model rats that were treated with AGNH after MCAO surgery. Briefly, 1892 DEGs were found after I/R, and 2164 DEGs were found after AGNH treatment; among them, there were 1328 overlapping DEGs (Fig. 2A, Table S1). The gene expression pattern of AGNH-treated ischaemic rats was similar to that of sham-treated rats (Fig. 2B). Then, we performed enrichment analysis of the 1328 overlapping DEGs and found that these DEGs were enriched in GO terms that were involved in inflammation regulation, such as "inflammatory response", "regulation of cytokine production" and "immune effector process", and other GO terms, such as "response to wounding", "regulation of vasculature development", "vasculature development" and "extracellular matrix organization". Then, the DEGs enriched in the GO term "inflammatory response" were analysed, and a network was constructed (Fig. 2C). Among the network, the top 8 targets, including Tyrobp, Syk, Tlr2, Myd88, Ccl2, Mmp2, Lyn and Fn1, were identified as core targets since they had the largest degree in the network (Fig. 2D). The DEGs in the network were involved in inflammation-related KEGG pathways such as "toll-like receptor signalling pathway" and "NF-kappa B signalling pathway" (Fig. 2E).

Metabolomics Analysis

To reveal the metabolic changes, metabonomic analysis was performed, and OPLS-DA was used to analyse the results of various treatments (Fig. 3). The DMs are listed in Table S2. As indicated by Fig. 3A, MCAO surgery caused 201 upregulated DMs and 168 downregulated DMs. In contrast, AGNH treatment significantly upregulated 102 DMs and downregulated 68 DMs. A distinct separation was found in the metabolic profiles between I/R and sham and between I/R + AGH and I/R in the positive mode, and the Q2 (cum) values were 0.816 and 0.601, respectively. Additionally, the metabolic profiles between I/R + AGH and I/R in negative mode were also clearly separated with Q2 (cum) values of 0.887 and 0.606, respectively. Further analysis showed that the 13 enriched metabolite pathways between I/R vs. sham including purine metabolism, arginine biosynthesis, alanine, aspartate and glutamate metabolism, arginine and proline metabolism, glycerophospholipid metabolism, citrate cycle (TCA cycle), pyrimidine metabolism, ascorbate and aldarate metabolism, glycine, serine and threonine metabolism, glyoxylate and dicarboxylate metabolism, galactose metabolism, glutathione metabolism and biosynthesis of cofactors. And 11 enriched signalling pathways were found between I/R + AGH vs. I/R, including alanine, aspartate and glutamate metabolism, cysteine and methionine metabolism, sphingolipid metabolism, arginine biosynthesis, sulphur metabolism, histidine metabolism, arginine and proline metabolism, butanoate metabolism, aminoacyl-tRNA biosynthesis, glycerophospholipid metabolism and citrate cycle (TCA cycle) (Fig. 3D).

Integrating Data from Transcriptomics Analysis and Metabolomics Analysis

There were four important metabolic pathways identified by integrating data from transcriptomics analysis and metabolomics analysis including TCA, histidine metabolism, glycerophospholipid metabolism, urea cycle and metabolism of arginine, proline, glutamate, aspartate and asparagine (Fig. 4A–D). Further analysis indicated that the DEGs in the identified metabolic pathways were closely associated with the DEGs enriched in inflammatory response (Fig. 4E). Importantly, 8 key DMs such as L-histidine, 1-methylhistamine in histidine metabolism, L-serine in glycerophospholipid metabolism, and L-alanine, fumaric acid, malic acid, 1-pyrroline-4-hydroxy-2-carboxylate and N-(L-arginino) succinate in the pathway of urea cycle and metabolism of arginine, proline, glutamate, aspartate and asparagine and TCA were regulated by AGNH (Fig. 4F). Among these DMs, AGNH obviously increased the levels of L-histidine, L-serine, L-alanine, fumaric acid, malic acid and N-(L-arginino) succinate ($p < 0.05$) while decreased the levels of 1-pyrroline-4-hydroxy-2-carboxylate and 1-methylhistamine ($p < 0.05$).

AGNH Decreased Tyrobp/Syk, TRL2/Myd88 and Inhibited NF-κB Signalling Pathway in MCAO Model Rats

To validate the results from multi-omics analysis, the expression levels of Tyrobp, Syk, Tlr2, Myd88 and Ccl2 were determined. The mRNA expression levels of Tyrobp, Syk, Tlr2, Tlr7, Myd88 and Ccl2 were increased in MCAO model rats,

whereas these mRNA expression levels were significantly decreased after ANGH treatment (Fig. 5A). In addition, the MCAO rats displayed an obvious increase in Tyrobp, Syk, Tlr2, Myd88 and Ccl2 protein levels. In contrast, after treatment with AGNH, Tyrobp, Syk, Tlr2, Tlr7, Myd88 and Ccl2 protein levels were significantly reduced in MCAO model rats (Fig. 5B). And the protein level of Tlr7 was not reduced by AGNH treatment. As indicated by the Pearson analysis, the targets of Tyrobp, Syk and Tlr2 were significantly negative correlated with the levels of L-histidine, N-(L-arginino) succinate, fumaric acid and malic acid, and Tyrobp, Tlr2 and MYD88 was positively correlated with

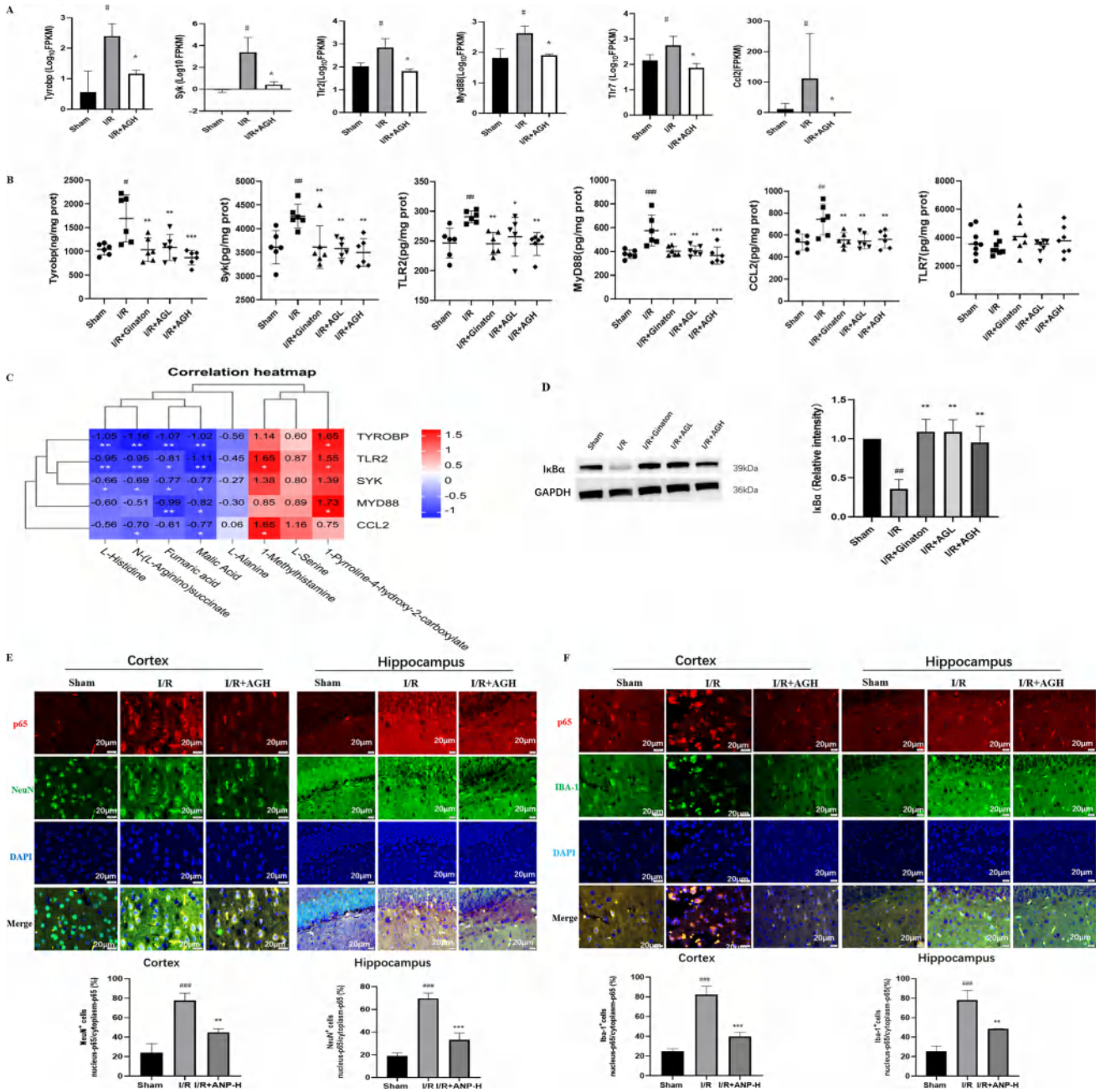

Fig. 5 The effect of AGNH on the expression of Tyrobp, Syk, Tlr2, Tlr7, Myd88 and Ccl2 in MCAO rats. **A** RNA-seq results of Tyrobp, Syk, Tlr2, Tlr7, Myd88 and Ccl2 ($n=3$); **B** ELISA of Tyrobp, Syk, Tlr2, Myd88, Tlr7 and Ccl2 ($n=6$); **C** the Pearson analysis of critical targets and critical metabolites, **D** western blotting results of IκBα ($n=3$), **E** IF staining of p65 (red) and NeuN (green) and the calculated nucleus p65/cytoplasm p65 of neurons in brain cortex and hippocampus ($n=3$); **F** IF staining of P65 (red) and Iba-1 (green) and the calculated nucleus p65/cytoplasm p65 of microglia in brain cortex and hippocampus ($n=3$), scale bar: 20 μm; $^{###}p<0.001$, $^{##}p<0.01$,$^{#}p<0.05$ vs. sham; $^{*}p<0.05$, $^{**}p<0.01$, $^{***}p<0.001$ vs. I/R group

the levels of 1-pyrroline-4-hydroxy-2-carboxylate, indicating the target was closely associated with the levels of the metabolites (Fig. 5C). Besides, MCAO rats displayed a significant decrease of IκBα, and this was remarkably increased by AGNH (Fig. 5D). IF staining results showed that MCAO surgery caused an obvious nucleus translocation of p65 in both brain cortex and hippocampus (Fig. 5E, F). In contrast, AGNH treatment significantly reduced the nucleus translocation of p65 in neuron in both brain cortex and hippocampus (Fig. 5E). Additionally, the nucleus translocation of p65 in microglia was also decreased in cortex and hippocampus after AGNH treatment (Fig. 5F). These results suggested that AGNH inhibited NF-κB signalling pathway in MCAO rats.

AGNH Inhibited Neuroinflammation, Cell Apoptosis and Improved Rat Movement Activity

MCAO-induced I/R model rats displayed a sharp increase of IL-1β, KC-GRO and TNF-α levels and a reduction of IL-10 levels. In contrast, AGNH treatment significantly decreased IL-1β, KC-GRO, IL-13 and TNF-α in I/R model rats (Fig. 6A, B). Additionally, IF results of cleaved caspase 3 indicated that MCAO surgery caused a sharp increase in cleaved caspase 3 and AGNH treatment significantly decreased cleaved caspase 3 in MCAO rats (Fig. 6C). Moreover, the MCAO rats displayed a decrease in the distance and time of the rat activity, and these were also improved after treatment with AGNH (Fig. 6D). These data suggested that ANGH inhibited neuroinflammation and cell apoptosis, and improved activities of MCAO rats.

Network Pharmacology Analysis Identified Potential Critical Components in AGNH

To identify the potential critical components in AGNH, a heterogeneous network of components-drug target-DEGs was constructed by using network pharmacological analysis and presented as Fig. 7. And 51 components (purple diamonds) were identified to affect 139 DEGs in biological process of inflammatory response (blue nodes) and DEGs in identified metabolic pathways (dark blue nodes) of TCA, histidine metabolism, glycerophospholipid metabolism, urea cycle and metabolism of arginine, proline, glutamate, aspartate and asparagine, through 140 drug targets (green nodes). Among these 51 components, top 10 components in degree were quercetin, wogonin, beta-sitosterol, baicalein, naringenin, acacetin, berberine and epiberberine, palmatine and berlambine, which were predicted to have an effect in reducing cerebral ischaemic infarct. Specifically, baicalin and berberine was used to control the quality of AGNH based on the regulations of AGNH pill in 2020 Chinese pharmacopoeia, and these two components can be found in rat plasma after intragastrical administration of AGNH (Fig. S1-S2). Thus, multiple components including quercetin, wogonin, beta-sitosterol, baicalein, naringenin, acacetin, berberine and epiberberine, palmatine and berlambine in AGNH were predicted to have an effect in reducing ischaemic infarct.

Discussion

In this study, the neuroprotective effects of AGNH treatment on MCAO-induced IS rat model were evaluated, and then transcriptomic analysis and metabolomics analysis were integrated to elucidate the potential mechanism. Specifically, treatment with AGNH offered an important neuroprotection in MCAO rats. It revealed that AGNH inhibited Tyrobp/Syk and Tlr2/Myd88, as well as NF-κB signalling pathway and regulated 8 key metabolites, including L-histidine, L-serine, L-alanine, fumaric acid, malic acid, and N-(L-arginino) succinate, 1-pyrroline-4-hydroxy-2-carboxylate and 1-methylhistamine to attenuate neuroinflammation after IS (Fig. 8). Network pharmacology analysis identified 51 components including quercetin, beta-sitosterol, baicalein, naringenin, acacetin, berberine and palmatine to have potential effect in decreasing IS injury.

Inflammation is a vital factor affecting the pathogenesis of IS, and it aggravates brain damage. During an IS, microglial activation triggers the overproduction of IL-1β and TNF-α, thus leading to neuronal loss and brain structure destruction [22, 23]. Additionally, inflammation is intertwined with excessive oxidative stress, BBB destruction, energy supply disorder and excitotoxicity, which makes ischaemic damage complicated and dangerous [24]. Notably, if local inflammation continues after IS, it causes long-term whole brain inflammation and continues to have an impact on neurological function recovery in IS patients. In this study, ischaemic rats induced by MCAO surgery displayed a sharp elevation of IL-1β, TNF-α and KC-GRO levels. In contrast, AGNH obviously reduced IL-1β, IL-13, TNF-α and KC-GRO levels in ischaemic rats, indicating the inhibitory effect of AGNH on inflammation after IS.

Tyrobp, also named DAP12, is expressed in microglia in the brain and has an immunoreceptor phosphotyrosine-based activation motif (ITAM) that interacts with receptors such as Trem2 and Trem1 [25]. Tyrobp can drive the phenotype changes of microglial [26, 27]. Tyrobp knockout in PSEN1G378E mice promoted learning behaviour recovery, reduced microglia number and decreased IL-6, IL-1β and TNF-α in the hippocampus [28]. Importantly, Tyrobp is coupled with Syk and Card9, which trigger IL-1a/b secretion [29]. As a nonreceptor tyrosine kinase, Syk transduces signals by recognizing ITAM domains in Tyrobp to mediate various types of acute or chronic inflammation, and inhibition of Syk decreased brain damage and IS-induced

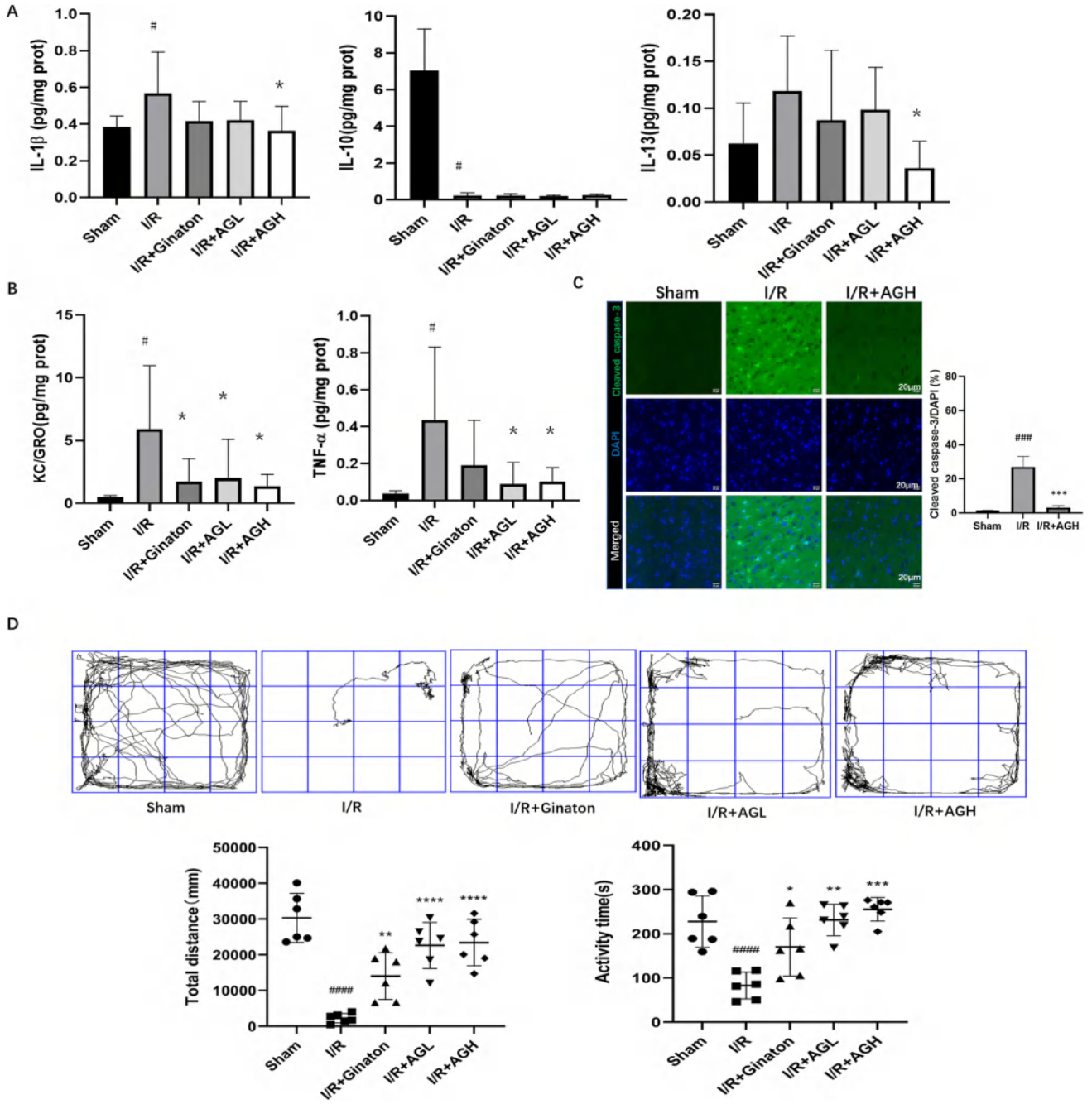

Fig. 6 AGNH decreased multiple inflammation factors and increased rat activity after I/R. **A** Levels of IL-1β, IL-10, and IL-13 ($n=6$–8), **B** KC-GRO and TNF-α ($n=6$–8); **C** IF of cleaved caspase 3 (green) and nuclei (blue) and the quantification of cleaved caspase 3 ($n=3$), scale bar: 20 μm; **D** open field test ($n=6$); $^{\#\#\#}p<0.001$, $^{\#}p<0.05$ vs. sham; $^{*}p<0.05$, $^{**}p<0.01$, $^{***}p<0.001$ vs. I/R group

neuroinflammation in a MCAO model [30]. In addition, mice treated with a Syk inhibitor showed lower infarction and improved neurological outcomes in an arterial thrombosis model [31]. In our study, AGNH obviously decreased Tyrobp and Syk levels and significantly inhibited ICAM-1, IL-1β, TNF-α and IL-13.

Toll-like receptors (TLRs) play important roles in in nonspecific immunity (innate immunity) and lead to downstream proinflammatory cytokine release as well as apoptotic cell death following IS [32]. As a major member of the TLR family, Tlr2 is increased after cerebral I/R; knockout of Tlr2 decreased inflammatory cell accumulation and promoted neuronal survival in C57 mice with cerebral ischaemia [33]. In particular, Tlr2 can bind Myd88 and lead to the activation of the downstream NF-κB signalling pathway and the secretion of IL-6 and IL-1β [32]. Moreover, recent research showed

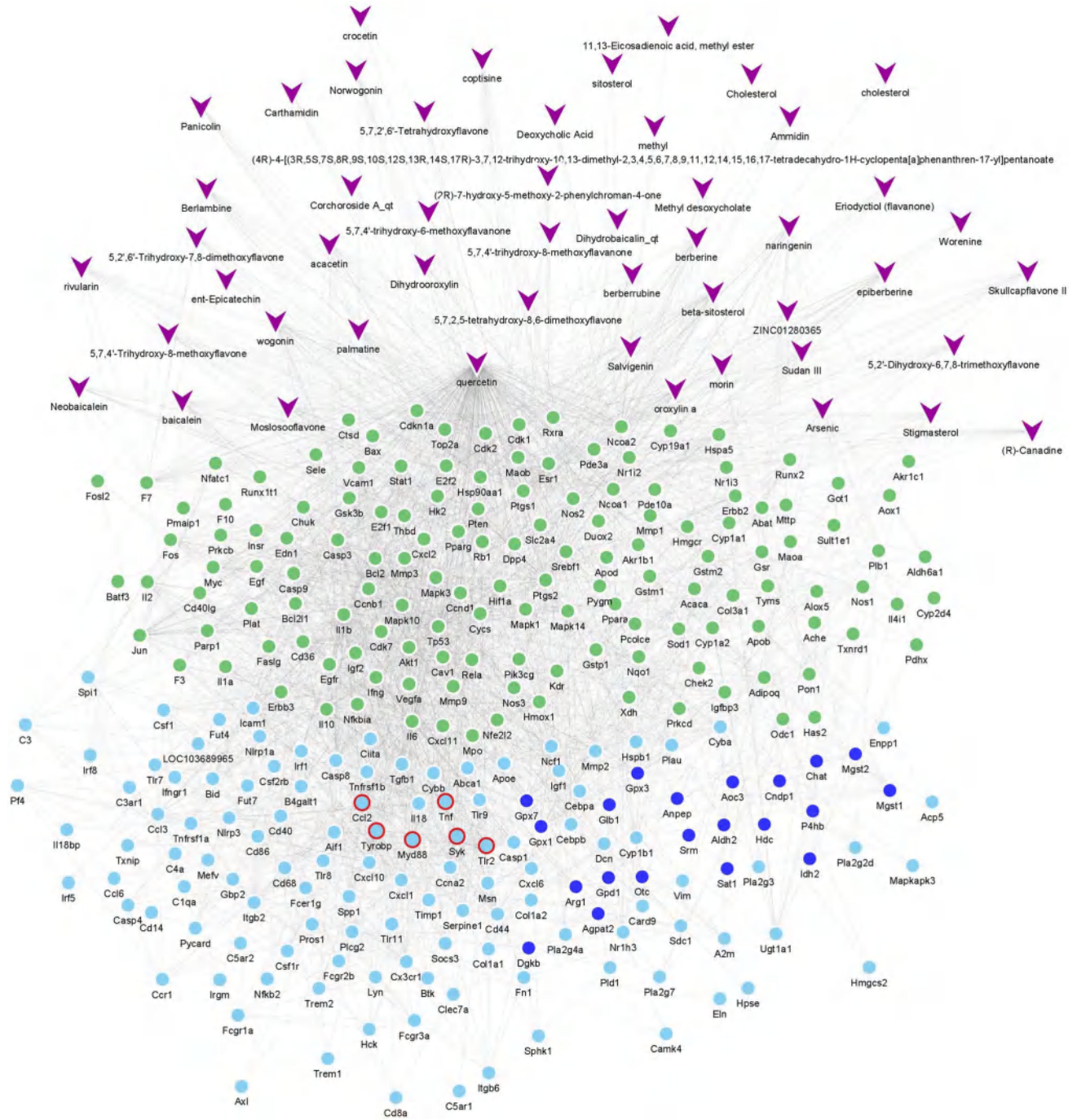

Fig. 7 Heterogeneous network of potential active components-drug target-DEGs by using network pharmacology analysis, purple diamonds, green nodes, blue nodes and dark blue nodes indicated components, drug targets, DEGs in inflammatory response and DEGs in metabolic pathways of TCA, histidine metabolism, glycerophospholipid metabolism, urea cycle and metabolism of arginine, proline, glutamate, aspartate and asparagine, respectively

that high Ccl2 levels were observed in MCAO model rats, and CCL2 inhibitors decreased the ischaemic infarct area and inflammatory response [34]. In our study, Tlr2 and Myd88 were also identified as vital targets in AGNH-mediated neuroprotection in multi-omics analysis. The high expression levels of Tlr2, Myd88 and Ccl2 in MCAO model rats were obviously reduced by AGNH. These signalling pathways may be mediated by inflammatory pathways such as the NF-κB signalling pathway, which were observed in the RNA-seq analysis. Additionally, the WB and IF experiments indicated that AGNH decreased nuclei location of p65 and increased IκBα level, which is a negative regulator of NF-κB signalling pathway.

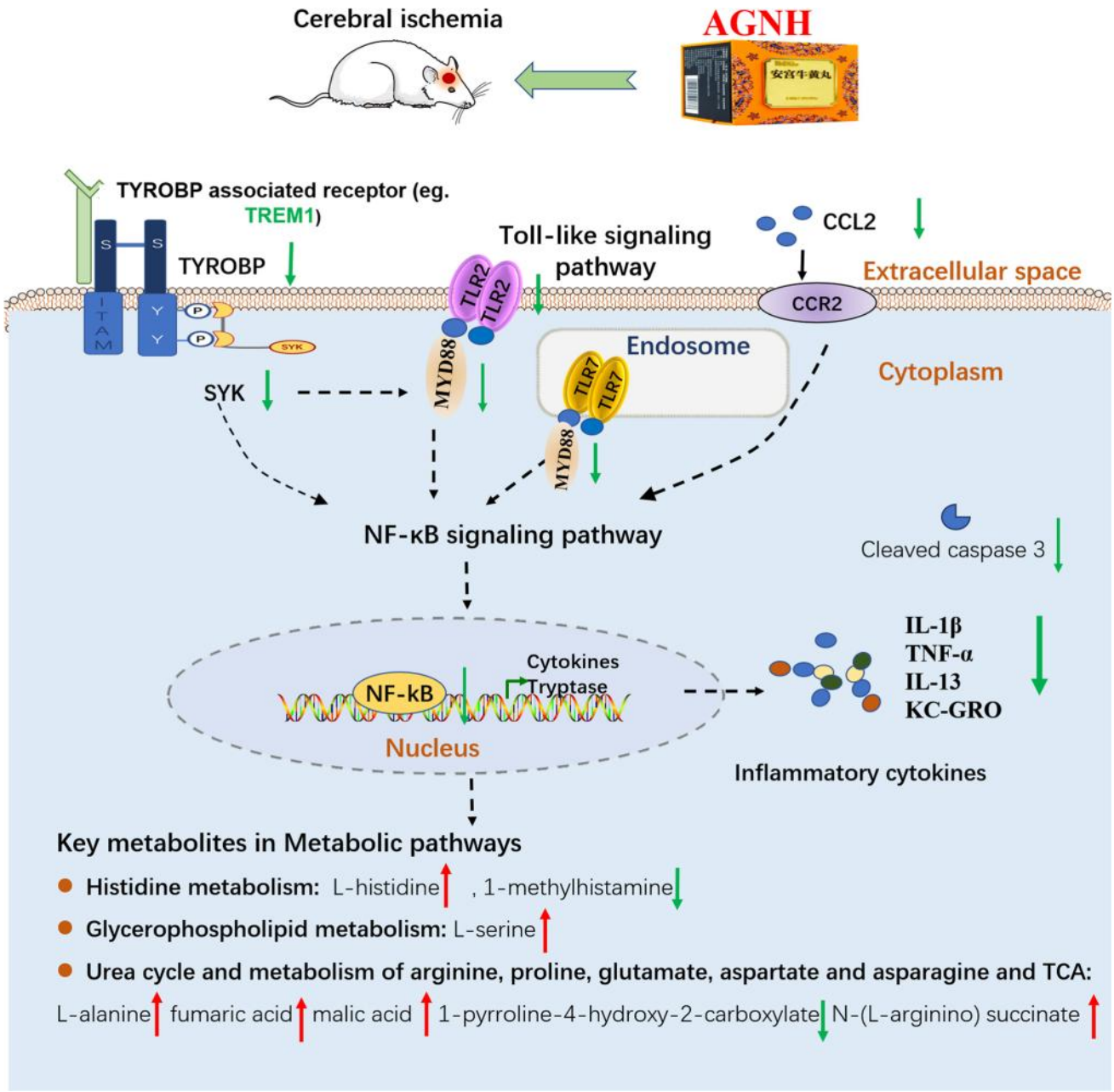

Fig. 8 Overview of the potential mechanism of AGNH in cerebral ischaemia

All these results demonstrated AGNH inhibited NF-κB signalling pathway to prevent the inflammatory response.

By integrating transcriptomics and metabolomics analysis, we identified 8 key metabolites including L-histidine, 1-methylhistamine, in histidine metabolism, L-serine, in glycerophospholipid metabolism, and L-alanine, fumaric acid, malic acid, 1-pyrroline-4-hydroxy-2-carboxylate and N-(L-arginino) succinate in the pathway of urea cycle and metabolism of arginine, proline, glutamate, aspartate and asparagine and TCA as vital DMs in the protection of AGNH against I/R injury (Fig. 4). In our study, an increase of L-histidine, L-serine, L-alanine, fumaric acid, malic acid and N-(L-arginino) succinate and a decrease of 1-methylhistamine and 1-pyrroline-4-hydroxy-2-carboxylate were observed after AGNH treatment. As a common amino acid, L-histidine exerted a good anti-oxidant and anti-inflammatory effect [35]. And 1-methylhistamine (MHA) was produced by the action of histamine-N-methyltransferase (HNMT) from histidine and was supposed to be a biomarker of histamine intolerance [36]. Studies have shown that L-serine decreased inflammatory responses by regulating macrophages and neutrophils in *Pasteurella multocida* infection [37], and treatment of traumatic brain injury with L-serine reduced

inflammatory responses and provided neuroprotection in mice [38]. L-alanine prevented pancreatic beta cells from inflammation-induced apoptosis [39]. As an intermediate product in the metabolic pathway of the citric acid cycle, fumaric acid and its esters are used to inhibit inflammation in the treatment of psoriasis [40, 41]. Moreover, L-malic acid reduces inflammation in myocardial I/R injury [42]. Additionally, N-(L-arginino) succinate is a precursor for arginine, which was proved to have neuroprotective effect against cerebral I/R [43]. Importantly, the elevated levels of L-histidine, L-serine, L-alanine, fumaric acid and malic acid may take part in inhibition inflammatory response in AGNH-mediated neuroprotection in cerebral I/R.

To identify the potential critical components in AGNH, a heterogeneous network of components-drug target-DEGs was constructed by using network pharmacological analysis and 51 components were identified to affect inflammatory response and metabolic pathways of TCA, histidine metabolism, glycerophospholipid metabolism, urea cycle and metabolism of arginine, proline, glutamate, aspartate and asparagine. Importantly, 7 of the top 10 components in degree were reported to decrease cerebral ischaemic infarct and protect against cerebral ischaemic injury, such as quercetin [44, 45], beta-sitosterol [46], baicalein [47], naringenin [48], acacetin [49], berberine [50, 51] and palmatine [52]. Thus, multiple components including quercetin, beta-sitosterol, baicalein, naringenin, acacetin, berberine and palmatine may play an important role in reducing ischaemic infarct.

Conclusion

AGNH exerted an important neuroprotection on the rats with cerebral ischaemic damage. AGNH decreased Tyrobp/Syk and Tlr2/Myd88 levels to inhibit NF-κB signalling and regulated 8 key metabolites such as L-histidine, 1-methylhistamine, L-serine, L-alanine, fumaric acid, malic acid, 1-pyrroline-4-hydroxy-2-carboxylate and N-(L-arginino) succinate to attenuate neuroinflammation and protect against IS. And network pharmacology analysis predicted that multiple components including quercetin, beta-sitosterol, baicalein, naringenin, acacetin, berberine and palmatine in AGNH may play an important role in protecting against IS. This study helps the clinical application of AGNH in IS treatment and deepens the understanding of its potential mechanism.

Supplementary Information The online version contains supplementary material available at https://doi.org/10.1007/s12035-024-04016-8.

Acknowledgements We are grateful for the professor for Yanan Sun for her technical support.

Author Contribution Jingjing Zhang: data curation, analysis, conceptualization, funding acquisition, investigation, writing—original draft; Liangliang Tian, Guangzhao Cao: data curation, investigation, visualization, software, validation; Xiaotong Zhu, Lihan Wang, Jingyi Hou, Yi Zhang, He Xu, Lixia Wang, Shicong Wang, Chen Zhao: data curation, investigation; Hongjun Yang: conceptualization, supervision, writing—review and editing. All data were generated in-house, and no paper mill was used. All authors agree to be accountable for all aspects of work ensuring integrity and accuracy.

Funding The authors would like to acknowledge the financial support from the National Natural Science Foundation of China (81974550), Scientific and Technological Innovation Project of China Academy of Chinese Medical Science (CI2021A04612, CI2021B017-03) and Fundamental Research Funds for the Central Public Welfare Research Institutes (ZZ13-YQ-046, ZXKT21007 and ZXKT23019).

Data Availability All data supporting described findings can be obtained from the corresponding authors upon reasonable request.

Declarations

Ethics Approval All animal experiments were approved by Ethics Committee of Animal Care and Use of the Institute of Basic Theories for Chinese Medicine, Chinese Academy of Chinese Medical Sciences (No: IBTCMCACMS21-2203–05).

Consent to Participate Not applicable.

Consent for Publication Not applicable.

Competing Interests The authors declare no competing interests.

References

1. Feigin VL, Forouzanfar MH, Krishnamurthi R, Mensah GA, Connor M, Bennett DA et al (2014) Global and regional burden of stroke during 1990–2010: findings from the Global Burden of Disease Study 2010. Lancet 383(9913):245–254. https://doi.org/10.1016/S0140-6736(13)61953-4
2. Minnerup J, Sutherland BA, Buchan AM, Kleinschnitz C (2012) Neuroprotection for stroke: current status and future perspectives. Int J Mol Sci 13(9):11753–11772. https://doi.org/10.3390/ijms130911753
3. Shi H, Liu KJ (2007) Cerebral tissue oxygenation and oxidative brain injury during ischemia and reperfusion. Front Biosci 12:1318–1328. https://doi.org/10.2741/2150
4. Chamorro A, Dirnagl U, Urra X, Planas AM (2016) Neuroprotection in acute stroke: targeting excitotoxicity, oxidative and nitrosative stress, and inflammation. Lancet Neurol 15(8):869–881. https://doi.org/10.1016/S1474-4422(16)00114-9
5. Shi K, Tian DC, Li ZG, Ducruet AF, Lawton MT, Shi FD (2019) Global brain inflammation in stroke. Lancet Neurol 18(11):1058–1066. https://doi.org/10.1016/S1474-4422(19)30078-X
6. Hou J, Cao G, Tian L, Zhou R, Zhang Y, Xu H, Wu HW, Wang LF, Yang HJ, Zhang JJ (2022) Integrated transcriptomics and metabolomics analysis reveals that C3 and C5 are vital targets of DuZhi Wan in protecting against cerebral ischemic injury. Biomed Pharmacother 155:113703. https://doi.org/10.1016/j.biopha.2022.113703
7. Sun K, Fan J, Han J (2015) Ameliorating effects of traditional Chinese medicine preparation, Chinese materia medica and active compounds on ischemia/reperfusion-induced cerebral microcirculatory disturbances and neuron damage. Acta Pharm Sin B 5(1):8–24. https://doi.org/10.1016/j.apsb.2014.11.002
8. Zhang J, Zhou R, Xiang C, Fan F, Gao J, Zhang Y et al (2020) Enhanced thioredoxin, glutathione and Nrf2 antioxidant systems by safflower extract and aceglutamide attenuate cerebral

ischaemia/reperfusion injury. J Cell Mol Med 24(9):4967–4980. https://doi.org/10.1111/jcmm.15099
9. Zhang J, Zhou R, Cao G, Zhang Y, Xu H, Yang H (2022) Guhong injection prevents ischemic stroke-induced neuro-inflammation and neuron loss through regulation of C5ar1. Front Pharmacol 13:818245. https://doi.org/10.3389/fphar.2022.818245
10. Yang X, Wang L, Li J, Liang N, Wang Y, Liu J (2018) Chinese herbal medicine Dengzhan Shengmai capsule as adjunctive treatment for ischemic stroke: a systematic review and meta-analysis of randomized clinical trials. Complement Ther Med 36:82–89. https://doi.org/10.1016/j.ctim.2017.12.004
11. Cai Y, Zhang X, Huang Y, Wang L, Sun J, Liang W et al (2019) The add-on effect of dengzhan shengmai capsules on secondary prevention of ischemic stroke: a multicentre, randomised, placebo-controlled clinical trial. Complement Ther Med 46:189–194. https://doi.org/10.1016/j.ctim.2019.08.015
12. Commission CP (2015) Pharmacopoeia of the People's Republic of China p.879. Chinese Medical Science and Technology Press, Beijing
13. Bai X, GFF, Tong L, Yang HJ (2023) CiteSpace knowledge map analysis of Angong Niuhuang pills in recent 20 years. Zhongguo Zhong Yao Za Zhi, 48(5). https://doi.org/10.19540/j.cnki.cjcmm.20221025.501
14. Guo Y, Yan S, Xu L, Zhu G, Yu X, Tong X (2014) Use of angong niuhuang in treating central nervous system diseases and related research. Evid Based Complement Alternat Med 2014:346918. https://doi.org/10.1155/2014/346918
15. Liu H, Yan Y, Pang P, Mao J, Hu X, Li D, Zhou B, Shan H (2019) Angong Niuhuang pill as adjuvant therapy for treating acute cerebral infarction and intracerebral hemorrhage: a meta-analysis of randomized controlled trials. J Ethnopharmacol 237:307–313. https://doi.org/10.1016/j.jep.2019.03.043
16. Tsoi B, Chen X, Gao C, Wang S, Yuen SC, Yang D et al (2019) Neuroprotective effects and hepatorenal toxicity of Angong Niuhuang Wan against ischemia-reperfusion brain injury in rats. Front Pharmacol 10:593. https://doi.org/10.3389/fphar.2019.00593
17. Chen H, Luo Y, Tsoi B, Gu B, Qi S, Shen J (2022) Angong Niuhuang Wan reduces hemorrhagic transformation and mortality in ischemic stroke rats with delayed thrombolysis: involvement of peroxynitrite-mediated MMP-9 activation. Chin Med 17(1):51. https://doi.org/10.1186/s13020-022-00595-7
18. Zhang H, Hui X, Wang Y, Wang Y, Lu X (2022) Angong Niuhuang pill ameliorates cerebral ischemia/reperfusion injury in mice partly by restoring gut microbiota dysbiosis. Front Pharmacol 13:1001422. https://doi.org/10.3389/fphar.2022.1001422
19. Zhang J, Zhou R, Deng L, Cao G, Zhang Y, Xu H, Hou JY, Ju S, Yang HJ (2022) Huangbai liniment and berberine promoted wound healing in high-fat diet/streptozotocin-induced diabetic rats. Biomed Pharmacother 150:112948. https://doi.org/10.1016/j.biopha.2022.112948
20. Li X, Zhang D, Bai Y, Xiao J, Jiao H, He R (2019) Ginaton improves neurological function in ischemic stroke rats via inducing autophagy and maintaining mitochondrial homeostasis. Neuropsychiatr Dis Treat 15:1813–1822. https://doi.org/10.2147/NDT.S205612
21. Zhang J, Guo F, Zhou R, Xiang C, Zhang Y, Gao J et al (2021) Proteomics and transcriptome reveal the key transcription factors mediating the protection of Panax notoginseng saponins (PNS) against cerebral ischemia/reperfusion injury. Phytomedicine 92:153613. https://doi.org/10.1016/j.phymed.2021.153613
22. Latour LL, Kang DW, Ezzeddine MA, Chalela JA, Warach S (2004) Early blood-brain barrier disruption in human focal brain ischemia. Ann Neurol 56(4):468–477. https://doi.org/10.1002/ana.20199
23. Candelario-Jalil E, Yang Y, Rosenberg GA (2009) Diverse roles of matrix metalloproteinases and tissue inhibitors of metalloproteinases in neuroinflammation and cerebral ischemia. Neuroscience 158(3):983–994. https://doi.org/10.1016/j.neuroscience.2008.06.025
24. Neumann J, Riek-Burchardt M, Herz J, Doeppner TR, Konig R, Hutten H et al (2015) Very-late-antigen-4 (VLA-4)-mediated brain invasion by neutrophils leads to interactions with microglia, increased ischemic injury and impaired behavior in experimental stroke. Acta Neuropathol 129(2):259–277. https://doi.org/10.1007/s00401-014-1355-2
25. Haure-Mirande JV, Audrain M, Ehrlich ME, Gandy S (2022) Microglial TYROBP/DAP12 in Alzheimer's disease: transduction of physiological and pathological signals across TREM2. Mol Neurodegener 17(1):55. https://doi.org/10.1186/s13024-022-00552-w
26. Hickman S, Kingery ND, Ohsumi TK, Borowsky ML, Wang LC, Means TK et al (2013) The microglial sensome revealed by direct RNA sequencing. Nat Neurosci 16(12):1896–1905. https://doi.org/10.1038/nn.3554
27. Audrain M, Haure-Mirande JV, Mleczko J, Wang M, Griffin JK, St George-Hyslop PH et al (2021) Reactive or transgenic increase in microglial TYROBP reveals a TREM2-independent TYROBP-APOE link in wild-type and Alzheimer's-related mice. Alzheimers Dement 17(2):149–163. https://doi.org/10.1002/alz.12256
28. Li R, Lv ZY, Li YX, Li W, Hao YL (2022) Effects of TYROBP deficiency on neuroinflammation of a Alzheimer's disease mouse model carrying a PSEN1 p.G378E mutation. Chin Med Sci J 37(4):320–330. https://doi.org/10.24920/004059
29. Yasukawa S, Miyazaki Y, Yoshii C, Nakaya M, Ozaki N, Toda S et al (2014) An ITAM-Syk-CARD9 signalling axis triggers contact hypersensitivity by stimulating IL-1 production in dendritic cells. Nat Commun 5:3755. https://doi.org/10.1038/ncomms4755
30. Ye XC, Hao Q, Ma WJ, Zhao QC, Wang WW, Yin HH et al (2020) Dectin-1/Syk signaling triggers neuroinflammation after ischemic stroke in mice. J Neuroinflammation 17(1):17. https://doi.org/10.1186/s12974-019-1693-z
31. van Eeuwijk JM, Stegner D, Lamb DJ, Kraft P, Beck S, Thielmann I, Kiefer F, Walzog B, Stoll G, Nieswandt B (2016) The novel oral syk inhibitor, Bl1002494, protects mice from arterial thrombosis and thromboinflammatory brain infarction. Arterioscler Thromb Vasc Biol 36(6):1247–1253. https://doi.org/10.1161/ATVBAHA.115.306883
32. Tajalli-Nezhad, S, Karimian, M, Beyer, C, Atlasi MA, Azami Tameh, A (2019) The regulatory role of Toll-like receptors after ischemic stroke: neurosteroids as TLR modulators with the focus on TLR2/4. Cell Mol Life Sci, 76(3): p. 523–537. https://doi.org/10.1007/s00018-018-2953-2
33. Ziegler G, Freyer D, Harhausen D, Khojasteh U, Nietfeld W, Trendelenburg G (2011) Blocking TLR2 in vivo protects against accumulation of inflammatory cells and neuronal injury in experimental stroke. J Cereb Blood Flow Metab 31(2):757–766. https://doi.org/10.1038/jcbfm.2010.161
34. Li L, Lou W, Li H, Zhu Y, Huang X (2020) Upregulated C-C motif chemokine ligand 2 promotes ischemic stroke via chemokine signaling pathway. Ann Vasc Surg 68:476–486. https://doi.org/10.1016/j.avsg.2020.04.047
35. Vera-Aviles M, Vantana E, Kardinasari E, Koh NL, Latunde-Dada GO (2018) Protective role of histidine supplementation against oxidative stress damage in the management of anemia of chronic kidney disease. Pharmaceuticals (Basel) 11(4). https://doi.org/10.3390/ph11040111
36. Sánchez-Pérez S, Celorio-Sardà R, Veciana-Nogués MT, Latorre-Moratalla ML, Comas-Basté O, Vidal-Carou MC (2022) 1-Methylhistamine as a potential biomarker of food histamine intolerance. A pilot study. Front Nutr 9:973682. https://doi.org/10.3389/fnut.2022.973682

37. He, F, Yin, Z, Wu, C, Xia, Y, Wu, M, Li, , et.al. (2019) l-Serine lowers the inflammatory responses during Pasteurella multocida infection. Infect Immun, 87(12). https://doi.org/10.1128/iai.00677-19
38. Zhai P, Xu L, Yang J, Jiang Z, Zhao G, Sun L et al (2015) Reduction of inflammatory responses by L-serine treatment leads to neuroprotection in mice after traumatic brain injury. Neuropharmacology 95:1–11. https://doi.org/10.1016/j.neuropharm.2015.02.026
39. Cunningham GA, McClenaghan NH, Flatt PR, Newsholme P (2005) L-alanine induces changes in metabolic and signal transduction gene expression in a clonal rat pancreatic beta-cell line and protects from pro-inflammatory cytokine-induced apoptosis. Clin Sci (Lond) 109(5):447–455. https://doi.org/10.1042/CS20050149
40. Cordaro M, Casili G, Paterniti I, Cuzzocrea S, Esposito E (2017) Fumaric acid esters attenuate secondary degeneration after spinal cord injury. J Neurotrauma 34(21):3027–3040. https://doi.org/10.1089/neu.2016.4678
41. Gold R, Linker RA, Stangel M (2012) Fumaric acid and its esters: an emerging treatment for multiple sclerosis with antioxidative mechanism of action. Clin Immunol 142(1):44–48. https://doi.org/10.1016/j.clim.2011.02.017
42. Tang X, Liu J, Dong W, Li P, Li L, Lin C, Zheng Y, Hou J, Li D (2013) The cardioprotective effects of citric acid and L-malic acid on myocardial ischemia/reperfusion injury. Evid Based Complement Alternat Med 2013:820695. https://doi.org/10.1155/2013/820695
43. Chen SF, PM, Tang JC, Cheng J, Zhao D, Zhang Y, Liao HB, Liu R, Zhuang Y, Zhang ZF, Chen J, Lei RX, Li SF, Li HT, Wang ZF, Wan Q (2020) Arginine is neuroprotective through suppressing HIF-1α/LDHA-mediated inflammatory response after cerebral ischemia/reperfusion injury. Mol Brain, 13(1): p. 63. https://doi.org/10.1186/s13041-020-00601-9
44. Zhang L et al (2022) Neuroprotective effects of quercetin on ischemic stroke: a literature review. Front Pharmacol 13:854249. https://doi.org/10.3389/fphar.2022.854249
45. Cen J et al (2022) A water-soluble quercetin conjugate with triple targeting exerts neuron-protective effect on cerebral ischemia by mitophagy activation. Adv Healthc Mater 11(22):e2200817. https://doi.org/10.1002/adhm.202200817
46. Tang X et al (2024) Treatment with beta-sitosterol ameliorates the effects of cerebral ischemia/reperfusion injury by suppressing cholesterol overload, endoplasmic reticulum stress, and apoptosis. Neural Regen Res 19(3):642–649. https://doi.org/10.4103/1673-5374.380904
47. Li M et al (2022) Baicalein ameliorates cerebral ischemia-reperfusion injury by inhibiting ferroptosis via regulating GPX4/ACSL4/ACSL3 axis. Chem Biol Interact 366:110137. https://doi.org/10.1016/j.cbi.2022.110137
48. Bai X et al (2014) Protective effect of naringenin in experimental ischemic stroke: down-regulated NOD2, RIP2, NF-kappaB, MMP-9 and up-regulated claudin-5 expression. Neurochem Res 39(8):1405–1415. https://doi.org/10.1007/s11064-014-1326-y
49. Bu J et al (2019) Acacetin protects against cerebral ischemia-reperfusion injury via the NLRP3 signaling pathway. Neural Regen Res 14(4):605–612. https://doi.org/10.4103/1673-5374.247465
50. Zhu JR et al (2018) Berberine attenuates ischemia-reperfusion injury through inhibiting HMGB1 release and NF-kappaB nuclear translocation. Acta Pharmacol Sin 39(11):1706–1715. https://doi.org/10.1038/s41401-018-0160-1
51. Zhao L et al (2021) Berberine attenuates cerebral ischemia-reperfusion injury induced neuronal apoptosis by down-regulating the CNPY2 signaling pathway. Front Pharmacol 12:609693. https://doi.org/10.3389/fphar.2021.609693
52. Pereira JF et al (2023) Palmatine, a natural alkaloid, attenuates memory deficits and neuroinflammation in mice submitted to permanent focal cerebral ischemia. J Neuroimmunol 381:578131. https://doi.org/10.1016/j.jneuroim.2023.578131

Authors and Affiliations

Liangliang Tian[1] · Guangzhao Cao[1,2] · Xiaotong Zhu[1] · Lihan Wang[2] · Jingyi Hou[2] · Yi Zhang[1] · He Xu[1] · Lixia Wang[1] · Shicong Wang[3] · Chen Zhao[3] · Hongjun Yang[1,2] · Jingjing Zhang[1,4]

✉ Hongjun Yang
hongjun0420@vip.sina.com

✉ Jingjing Zhang
zjj4785@163.com

Liangliang Tian
llt0791@163.com

Guangzhao Cao
cgzbucm2020@163.com

Lihan Wang
lhwang29@163.com

Jingyi Hou
hjy_2016@126.com

Yi Zhang
zy701223@sina.com

He Xu
hxu@icmm.ac.cn

Lixia Wang
wanglxia95@163.com

Shicong Wang
pzhwsc@zzpzh.com

Chen Zhao
pzhzc@zzpzh.com

[1] Institute of Chinese Materia Medica, China Academy of Chinese Medical Sciences, Beijing 100700, China

[2] Experimental Research Center, China Academy of Chinese Medical Sciences, Beijing 100700, China

[3] Fujian Pien Tze Huang Enterprise Key Laboratory of Natural Medicine Research and Development, Zhangzhou 363000, Fujian, China

[4] Chinese Institute for Brain Research, Beijing 102206, China